

Electronic Supplementary Information for

Biomimetic Mimicry of Formaldehyde-Induced DNA-Protein Crosslinks in the Confined Space of Metal-Organic Framework

Yu-Bai Wei,^a Dong Luo,^a Xiao Xiong,^a Yong-Liang Huang,^b Mo Xie,^a Weigang Lu,^{*,a}
and Dan Li^{*,a}

[a] College of Chemistry and Materials Science, Guangdong Provincial Key Laboratory of Functional Supramolecular Coordination Materials and Applications, Jinan University, Guangzhou 510632, P. R. China

[b] Department of Chemistry, Shantou University Medical College, Shantou, Guangdong 515041, P. R. China

E-mail: weiganglu@jnu.edu.cn (W. L.); danli@jnu.edu.cn (D. L.)

Table of Contents

Experimental Section	S2
Materials and Instruments	S2
Synthesis of Crystals and Complexes	S2
Experimental Methods	S3
Structure Section	S6
Crystal Data and Structure Refinements	S6
Structural Analysis	S8
Characterization Section	S13
(Including UV-Vis spectra, excitation spectra, emission spectra, fluorescence lifetime, PXRD, IR, TGA, etc)	

Experimental Section

Materials and Instruments

All reagents and solvents were purchased from commercial sources and used without further purification. Thermogravimetric analyses (TGA) were performed on Thermo Scientific TGA 2 thermal analysis equipment under nitrogen flow of 20 mL min⁻¹ at a heating rate of 10 °C min⁻¹. ¹H-NMR and ¹³C-NMR spectra were recorded on Bruker AVANCE III HD 400 (400 MHz) equipment. ¹³C-SSNMR experiments were carried out on 14.1 T Advance Neo Bruker NMR spectrometer operating at a ¹³C frequency of 150 MHz, using a ramped 100 pulse with SPINAL64 for heteronuclear decoupling. Powder X-ray diffraction (PXRD) was performed on Rigaku Ultima IV diffractometer with Cu K α radiation ($\lambda = 1.5418 \text{ \AA}$) in a step of 0.02° under the tube conditions of 40 kV and 40 mA. Solid-state UV-Vis spectra were measured a Bio-Logic MOS-450/AF-CD Spectrometer. Infrared spectra were obtained by using KBr disks on Nicolet Avatar 360 FT-IR spectrometer in the range of 4000 – 400 cm⁻¹ (abbreviations for the IR bands: w = weak, m = medium, b = broad, and vs = very strong). HRESI-TOF mass spectra were measured on AB SCIEX X500R QTOF. The data analyses of ESI-TOF mass spectra were processed on SCIEXOS software. Elemental analyses were carried out on Elementar Vario Micro cube CHNS analyzer. Steady-state photoluminescence (PL) spectra were recorded on Horiba FluoroLog-3 fluorometer. Decay curves were recorded on an Edinburgh FLS920 spectrometer equipped with a NanoLED-370 flash lamp. Isothermal titration calorimetry (ITC) titration was carried out on Malvern MicroCal™ VP-ITC. The fluorescence photographs were taken under Olympus fluorescence microscope (Japan 163-0914), microscope model BX53F2, light source model TH4-200, fluorescence model U-RFL-T, digital camera model DP27, and software ST-ST-2.4. Scanning electron microscope (SEM) images were taken on M-30 PLUS Benchtop Scanning Electron Microscope (South Korea, COXEM Company). Supercritical CO₂ activation was conducted on samdri-PVT-3D (U.S.A., Tousimis Research Corporation Rockville). Gas adsorption were performed on Automatic Specific Surface Area and Micropore Physical and Chemical Adsorption Analyzer (ASAP 2020 PLUS) (USA, Micromeritics Instrument Corp.). H₂BPDC-(NH₂)₂ was synthesized according to our previous report.¹ The DNA picture in Scheme 1 has been re-produced using Servier Medical Art on <http://www.servier.com>.

Synthesis of Crystals and Complexes

Synthesis of JNU-101

A mixture of $\text{Zn}(\text{NO}_3)_2 \cdot 6\text{H}_2\text{O}$ (23.8 mg, 0.08 mmol), 2,6-diaminopurine (3.0 mg, 0.02 mmol), $\text{H}_2\text{BPDC}-(\text{NH}_2)_2$ (10.9 mg, 0.04 mmol), DMF/ H_2O (5 mL, 4.55/0.45, v/v), and nitric acid (68%, 0.01~0.02 mL) was introduced into a 25 mL of Parr Teflon-lined stainless steel vessel and heated at 135 °C for 3 days. After cooled to room temperature, the formed crystals (**JNU-101**) were filtered, washed with DMF, and air-dried (Yield: 12.1 mg, 32 %). IR (KBr pellet, cm^{-1}): 3343(s), 3211(m), 1652(m), 1594(s), 1551(w), 1473(w), 1385(s), 1291(w), 1254(w), 1223(m), 1161(m), 1099(w), 1003(w), 894(w), 788(s), 741(w), 656(w), 532(w). Elemental analysis (CHN), $\text{C}_{74}\text{H}_{92}\text{N}_{34}\text{O}_{26}\text{Zn}_6$ (including 4 DMF and 7 H_2O), calculated (%): C 39.43, H 4.11, N 21.13; found (%): C 39.35, H 4.12, N 21.33.

Synthesis of HCHO@JNU-101

The as-synthesized **JNU-101** was soaked in 1%, 5%, 10%, 15%, or 37% HCHO aqueous solutions for 1 day, and then washed with H_2O to afford **1%HCHO@JNU-101**, **5%HCHO@JNU-101**, **10%HCHO@JNU-101**, **15%HCHO@JNU-101**, or **37%HCHO@JNU-101**, respectively.

Experimental Methods

Isothermal Titration Calorimetry (ITC) Experiments

Blank experiments of the titration of buffer with HCHO solution and the titration of MOF suspension with buffer were first carried out to confirm the selected buffer doesn't interact with either of the titration components. In a typical titration, a HCHO solution was incrementally added into ITC sample cell containing an aqueous suspension of **JNU-101**. All titration experiments were performed in aqueous solutions without adjusting pH under the following conditions: reference power ($15 \mu\text{cal s}^{-1}$), initial injection delay (300 s), stirring speed (850 rpm), feedback mode gain (high feedback), spacing between injections (600-700 s), and filter period (10 s). All titration experiments were performed in triplicate and the averages were reported. The thermodynamic profile of each binding process was calculated by fitting the data with a single-site interaction model.

To set up an experimental run, the reference cell was filled with degassed deionized water and the sample cell was filled with **JNU-101** suspension. Upon completion of an experimental run,

the instrument was extensively cleaned before next use according to the following procedure: The reference cell was rinsed with water three times and with the buffer three times. The sample cell was soaked with a dilute hydrochloric acid (1.0 M) for 10 min three times. The sample cell was then rinsed with deionized water at least five times until no soap bubbles were observed in the syringe. Finally, the sample cell was rinsed three times with the buffer.

Fluorescence Titration Experiments

20 mg of **JNU-101** was finely ground into powders and then transferred in a 100 mL volumetric flask. Deionized water was added to the mark, and sonicated for 30 min to form a uniformly dispersed MOF suspension (0.20 mg mL^{-1}). To 2.70 mL of above suspension, add $20 \mu\text{L}$ HCHO solution (0.10 mM) incrementally to monitor the fluorescence emission intensity (excited at 365 nm) until the endpoint.

HCHO Crosslinking Interference Experiments

Gly: 0.25 M of glycine (Gly) aqueous solution, 0.36 M of HCHO aqueous solution, and **JNU-101** suspension (0.20 mg mL^{-1}) were prepared, respectively. The fluorescence emission of 2.7 mL of **JNU-101** suspension was recorded and taken as the blank. Then, $150 \mu\text{L}$ of HCHO solution was added to the above suspension, and the fluorescence emission of the resulting mixture was recorded. Following, $150 \mu\text{L}$ of Gly solution was added to the above mixture and its fluorescence emission was recorded again. Each experiment was repeated three times.

Tris: 0.10 M HCHO aqueous solution and the Tris solutions with different concentrations (0.12 M, 0.25 M, 0.60 M, and 0.75 M) were prepared, respectively. 0.12 M Tris solution was taken as an example. The fluorescence emission of 2.7 mL of **JNU-101** suspension was recorded and used as the blank, then $150 \mu\text{L}$ of HCHO solution was added, and its fluorescence emission was recorded. Next, $150 \mu\text{L}$ of Tris solution (0.12 M) was added to the above suspension, and the fluorescence emission of the resulting mixture was recorded again. Each experiment was repeated three times.

Metabolites: The following solutions were prepared first, HCHO (10 mM and 100 mM), urea (60 mM), formic acid (2.60 mM), methanol (0.20 M), vitamin C (0.78 mM), creatinine (14.70 mM), acetone (0.20 M), citric acid (4.06 mM), L-carnosine (0.10 mM), EtOH (0.20 M), L-carnitine (0.46 mM), acetic acid (0.20 M), glutathione (10 mM), D-lactic acid (11.98 mM), and maltose (0.06 mM). Then, the fluorescence emission of 2.70 mL of **JNU-101** suspension (0.20

mg mL⁻¹) was recorded and used as the blank. Finally, taking urea as an example, 0.30 mL of the above urea solution was added into 2.70 mL of an aqueous **JNU-101** suspension (0.20 mg mL⁻¹), and the fluorescence emission was recorded; or, 30 μ L of each of the above 15 metabolites were added into 2.55 mL of **JNU-101** aqueous suspension, and the fluorescence emission was recorded. The concentrations of the above metabolites were selected according to those in human serum or urine reported in references.

Amino acids: The following solutions of amino acids (each 50 mM) were prepared first, valine (Val), serine (Ser), phenylalanine (Phe), methionine (Met), histidine (His), alanine (Ala), and HCHO. Then, take Val as an example, the fluorescence emission of 2.70 mL of **JNU-101** suspension (0.20 mg mL⁻¹) was recorded and used as the blank. Next, 150 μ L of HCHO was added and its fluorescence intensity was recorded. Finally, 150 μ L of Val was added to the above suspension and its fluorescence emission was recorded again. Each experiment was repeated three times.

Fluorescence Imaging Studies

0.1 mM, 0.2 mM, and 0.4 mM HCHO solutions of cell culture medium (DMEM + 2% FBS) were prepared. The as-synthesized **JNU-101** was photographed with a fluorescence microscope in the bright field, and then under UV irradiation in the dark field. The above HCHO containing medium was added and incubated for 10 minutes, photographed again in the bright field and under UV irradiation in the dark field.

HCHO Vapor Detection Experiments

HCHO vapor detection experiment was performed on a setup previously reported by our group.² The **JNU-101** powder was pressed onto a quartz plate to form a thin film, and placed in a quartz cuvette with a capillary tube containing 1% HCHO solution. The cuvette was capped. The *in-situ* time-dependent fluorescence emission was measured.

Gas adsorption

The as-synthesized **JNU-101** was solvent exchanged with methanol and then transferred to a supercritical CO₂ instrument inside a glove box for solvent extraction procedure. Finally, the

JNU-101 after supercritical CO₂ activation was transferred to an adsorption tube, applied vacuum at room temperature, and conducted gas adsorption measurements.

Structure Section

Crystal Data and Structure Refinements

Single-crystal X-ray diffraction data collections were implemented on an Oxford Cryo stream system on a XtaLAB PRO MM007-DW diffractometer (Rigaku, Cu K α , $\lambda = 1.54184$ Å) equipped with a graphite monochromator and Pilatus3R-200K-A detector at 100 or 293 K. The Structures were solved using direct methods and refined with full-matrix least-squares refinements using the SHELX2018/3 programs. All non-hydrogen atoms were refined by anisotropic thermal parameters, and the hydrogen atoms were formed geometrically. Some of the guest molecules in **JNU-101** and **HCHO@JNU-101** were highly disordered and could not be located and refined successfully. SQUEEZE program of PLATON software was used to eliminate the scattering of guest molecules. Parameters for crystal data and refinements are summarized in **Table S1**. CCDC Nos. 2041867 for **JNU-101 (1)**, 2081107 for **1%HCHO@JNU-101 (2)**, 2081106 for **5%HCHO@JNU-101 (3)**, 2081103 for **10%HCHO@JNU-101 (4)**, 2081104 for **15%HCHO@JNU-101 (5)**, and 2081105 for **37%HCHO@JNU-101 (6)**.

Table S1. Crystal data and structure refinements for **1**, **2**, and **3**

Compounds	1	2	3
Empirical formula	C ₆₂ H ₅₀ N ₃₀ O ₁₅ Zn ₆	C ₆₄ H ₅₀ N ₃₀ O ₁₅ Zn ₆	C ₆₆ H ₅₀ N ₃₀ O ₁₅ Zn ₆
Formula weight	1847.54	1871.56	1895.58
Temperature/K	99.97(10)	100.01(12)	100(18)
Crystal system	monoclinic	monoclinic	monoclinic
Space group	<i>P2/c</i>	<i>P2/c</i>	<i>P2/c</i>
<i>a</i> /Å	20.6236(2)	20.5713(10)	20.5389(19)
<i>b</i> /Å	15.3773(10)	15.3320(4)	15.2128(5)
<i>c</i> /Å	21.8559(3)	21.6572(8)	21.6422(9)
<i>α</i> /°	90	90	90
<i>β</i> /°	98.0830	96.891	94.526
<i>γ</i> /°	90	90	90
Volume/Å ³	6862.42(12)	6781.3(5)	6741.1(7)
<i>Z</i>	2	2	2
$\rho_{\text{calc}}/\text{cm}^3$	0.896	0.917	0.934
μ/mm^{-1}	1.547	1.571	1.586
F(000)	1864.0	1888.0	1912.0
Radiation	Cu K α ($\lambda = 1.54184$)	Cu K α ($\lambda = 1.54184$)	Cu K α ($\lambda = 1.54184$)
Reflections collected	39963	36706	31357
Independent reflections	13872 [R _{int} = 0.0216]	10627 [R _{int} = 0.0561]	10879 [R _{int} = 0.0519]
Goodness-of-fit on F ²	1.024	0.965	1.058
Final R indexes [I ≥ 2σ (I)]	R ₁ = 0.0853 wR ₂ = 0.2584	R ₁ = 0.1114 wR ₂ = 0.2984	R ₁ = 0.1162 wR ₂ = 0.2985
Final R indexes [all data]	R ₁ = 0.0956 wR ₂ = 0.2706	R ₁ = 0.1781 wR ₂ = 0.3512	R ₁ = 0.1574 wR ₂ = 0.3476

$$^a R_1 = \Sigma(|F_o| - |F_c|) / \Sigma|F_o|; ^b wR_2 = [\Sigma w(F_o^2 - F_c^2)^2 / \Sigma w(F_o^2)^2]^{1/2}$$

Table S2. Crystal data and structure refinements for **4**, **5**, and **6**

Compounds	4	5	6
Empirical formula	C ₆₆ H ₅₀ N ₃₀ O ₁₅ Zn ₆	C ₆₆ H ₄₈ N ₃₀ O ₁₅ Zn ₆	C ₆₇ H ₅₀ N ₃₀ O ₁₅ Zn ₆
Formula weight	1895.58	1893.58	1907.59
Temperature/K	100(14)	100.00(10)	100(2)
Crystal system	monoclinic	monoclinic	monoclinic
Space group	<i>P2/c</i>	<i>P2/c</i>	<i>P2/c</i>
<i>a</i> /Å	20.7927(5)	20.7798(4)	20.6916(3)
<i>b</i> /Å	15.2180(2)	15.2345(2)	15.2813(2)
<i>c</i> /Å	21.7299(5)	21.6564 (4)	21.6745(3)
<i>α</i> /°	90	90	90
<i>β</i> /°	93.520	93.144	92.481
<i>γ</i> /°	90	90	90
Volume/Å ³	6862.9(2)	6845.4(2)	6846.94(16)
<i>Z</i>	2	2	2
ρ_{calc} /cm ³	0.917	0.920	0.925
μ /mm ⁻¹	1.558	1.562	1.564
F(000)	1912.0	1912.0	1924.0
Radiation	Cu K α (λ = 1.54184)	Cu K α (λ = 1.54184)	Cu K α (λ = 1.54184)
Reflections collected	38708	33429	36830
Independent reflections	12665 [R _{int} = 0.0422]	12586 [R _{int} = 0.0348]	11751 [R _{int} = 0.0338]
Goodness-of-fit on F ²	0.974	1.019	1.057
Final R indexes [I ≥ 2σ (I)]	R ₁ = 0.1002 wR ₂ = 0.2740	R ₁ = 0.0889 wR ₂ = 0.2611	R ₁ = 0.0929 wR ₂ = 0.2496
Final R indexes [all data]	R ₁ = 0.1408 wR ₂ = 0.3142	R ₁ = 0.1126 wR ₂ = 0.2925	R ₁ = 0.1091 wR ₂ = 0.2652

$$^a R_1 = \Sigma(|F_o| - |F_c|) / \Sigma|F_o|; ^b wR_2 = [\Sigma w(F_o^2 - F_c^2)^2 / \Sigma w(F_o^2)^2]^{1/2}$$

Structural Analysis

Topological analysis: a rigorous topological identification for the underlying topology of **JNU-101** was implemented by using the Systre and TOPOS programs. From the topological point of view, both BPDC-2NH₂ and 2,6-diaminopurine can be simplified as di-topic linkers and the two clusters as 4- and 6-connected nodes, respectively (**Fig. S1a** and **b**). Thus, the structure of **JNU-101** can be simplified as a (4,6)-*c* network with the point symbol of {4³.6².8}₂{4⁶.6⁶.8³}₂ and transitivity of [2473].

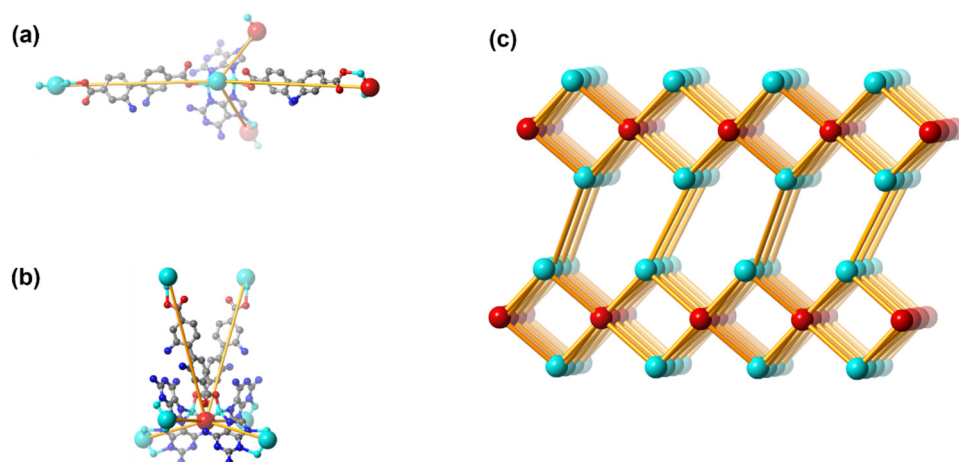


Figure S1. Topological simplification. (a) The quasi-paddle wheel dinuclear structure as a four-connected (4-c) node (cyan ball). (b) The two mononuclear structures linked through a $\mu_2\text{-O}^{2-}$ as a six-connected (6-c) node (red ball). (c) The underlying topology of **JNU-101**.

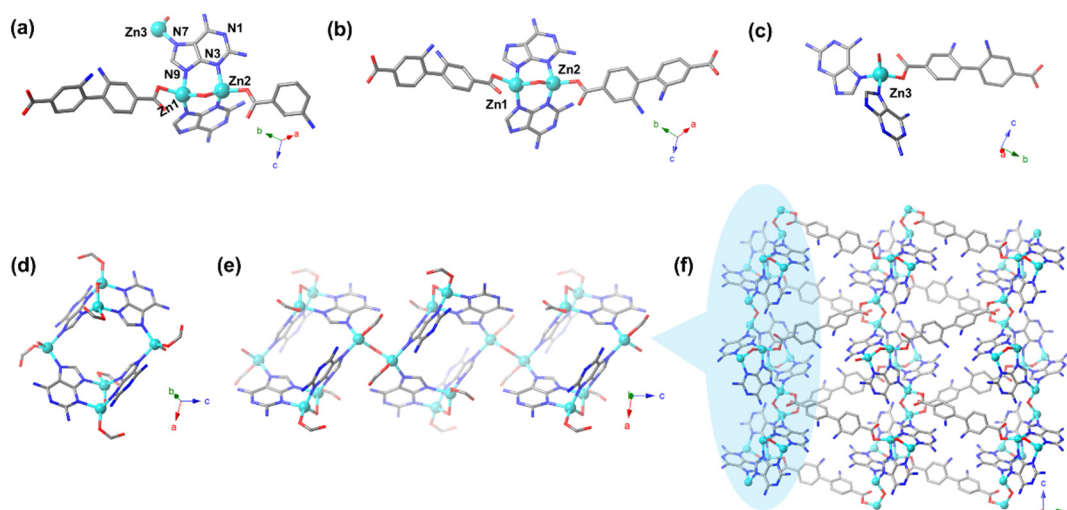


Figure S2. (a) Asymmetric unit of **JNU-101**. (b, c) Coordination environments of two Zn clusters in **JNU-101**. (d) A grid-like substructure composed of two clusters spaced by the backbone of diaminopurine. (e) Grid-like substructures linked through $\mu_2\text{-O}^{2-}$ forming a one-dimensional chain-like structure. (f) Adjacent one-dimensional chains extended through BPDC- 2NH_2 ligands forming a two-dimensional layer structure. Color codes: Zn, Cyan; C, grey; N, blue; O, red.

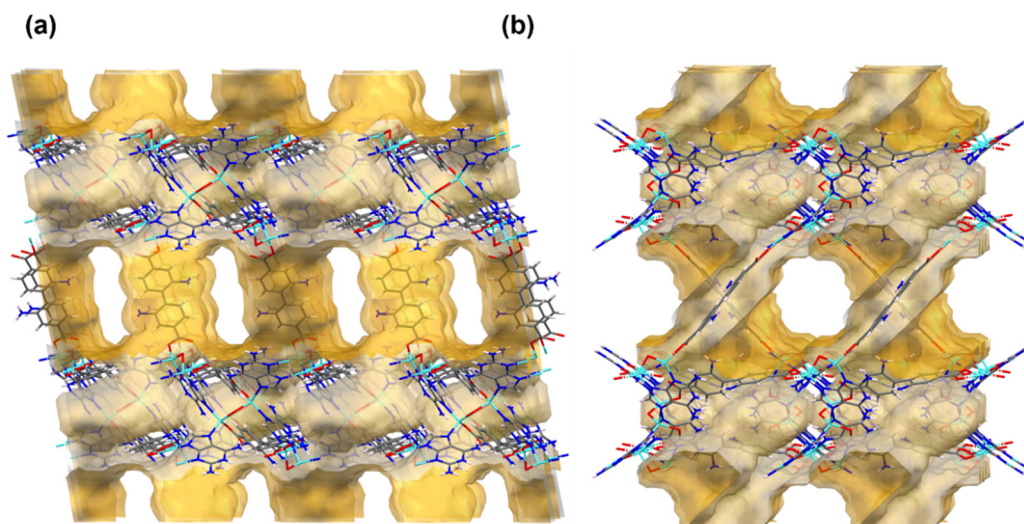


Figure S3. The surface of the channel in **JUN-101** along the *b* axis (a) and *c* axis (b), the probe molecule is 1.2 Å.

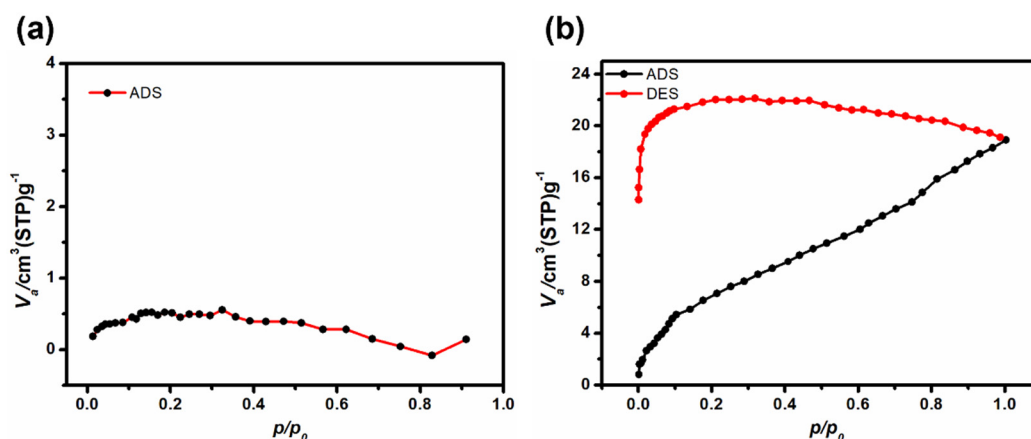


Figure S4. N₂ adsorption at 77 K (a) and CO₂ adsorption/desorption isotherms at 197 K (b) for **JNU-101** after supercritical CO₂ activation.

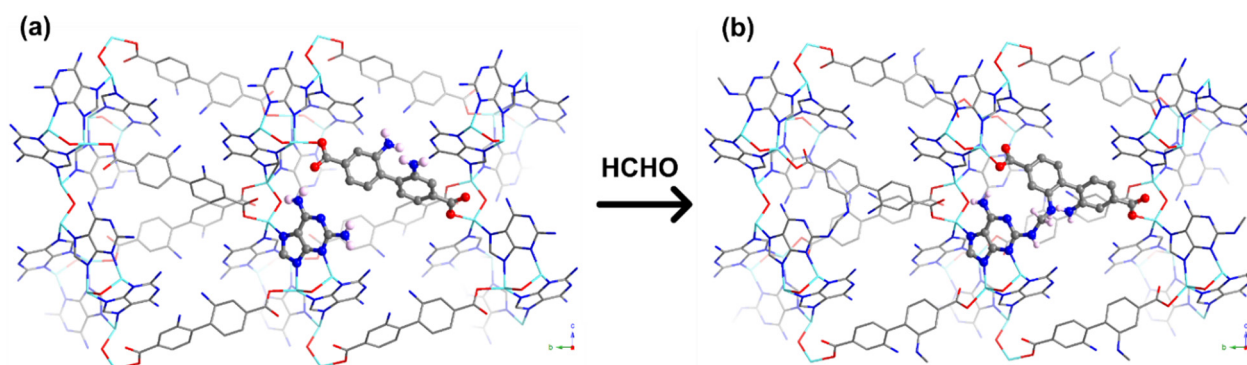


Figure S5. Two-dimensional (2D) layered structure of **1% HCHO@JNU-101** along the *a* axis; A pair of DAP and BPDC-2NH₂ are highlighted in ball-and-stick models showing the flipping of BPDC-2NH₂ before methylene knitting. Color codes: Zn, Cyan; C, grey; N, blue; O, red; H, pale pink.

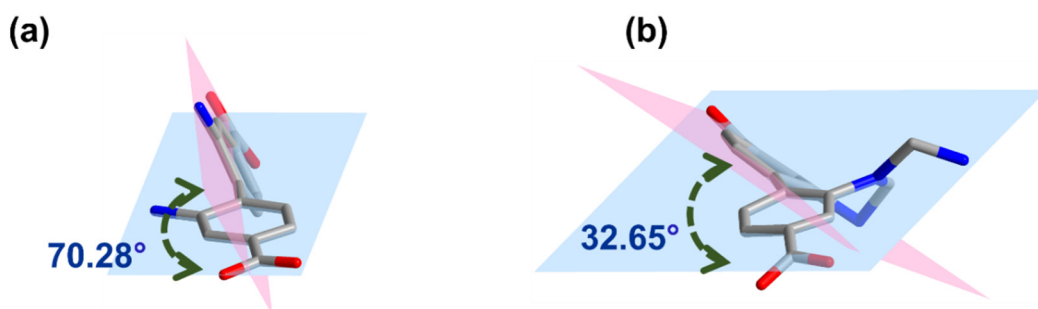


Figure S6. Torsional angles between the two benzene rings of BPDC-2NH₂ in **JNU-101** and **37%HCHO@JNU-101**.

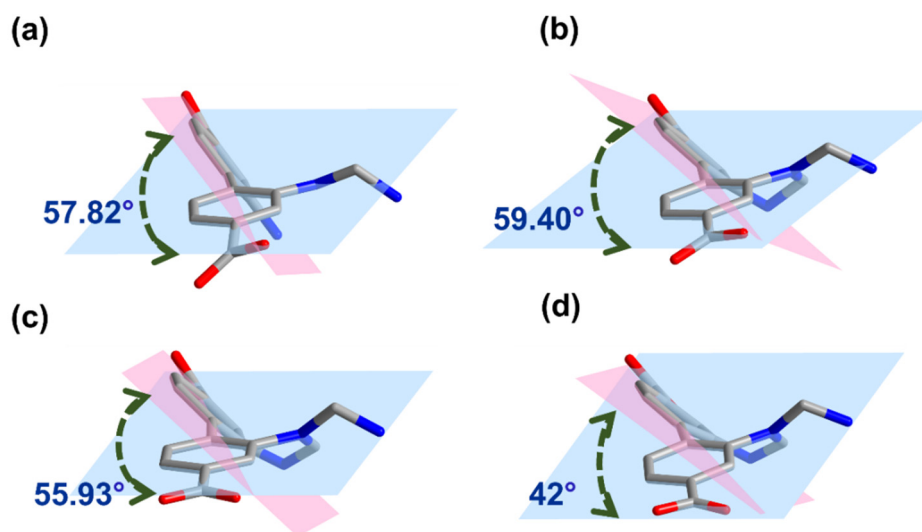


Figure S7. Torsional angles between the two benzene rings of BPDC-2NH₂ in **1%HCHO@JNU-101** (a); **5%HCHO@JNU-101** (b); **10%HCHO@JNU-101** (c); and **15%HCHO@JNU-101** (d).

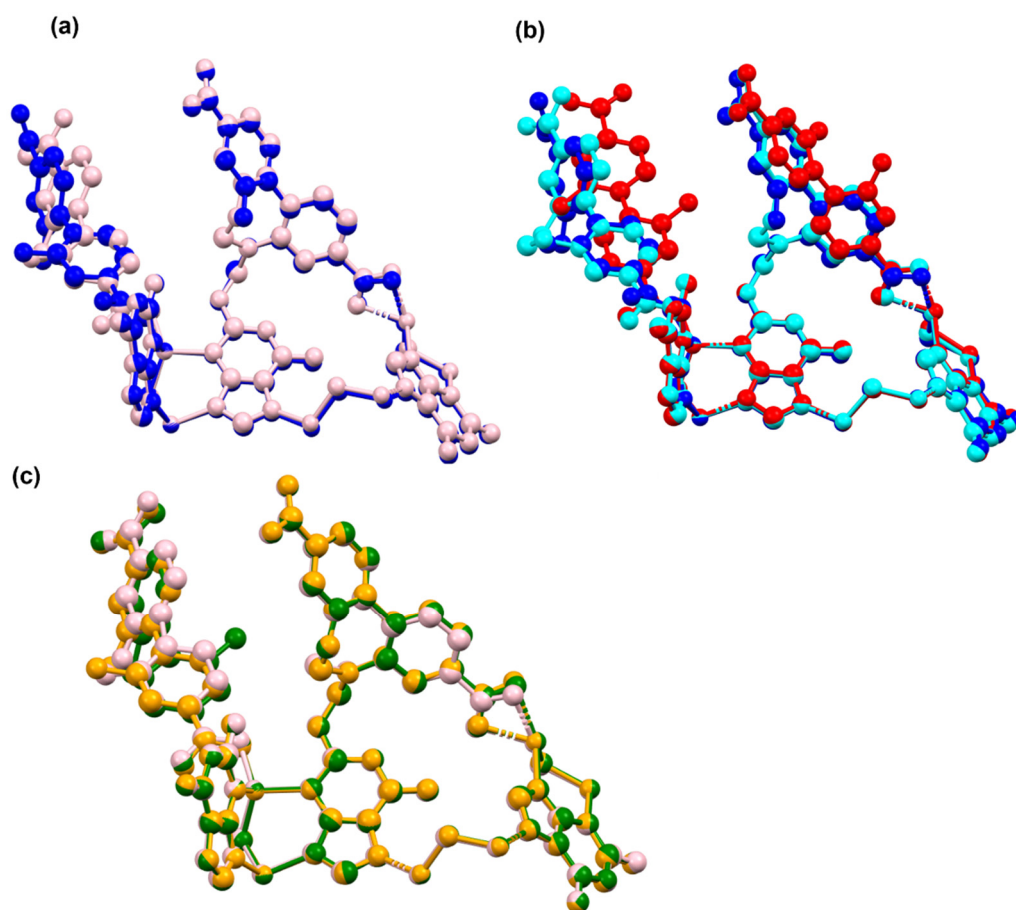


Figure S8. The local overlay of the crystal structure, **JNU-101** (red), **1%HCHO@JNU-101** (blue), **5%HCHO@JNU-101** (pink), **10%HCHO@JNU-101** (green), **15%HCHO@JNU-101** (orange); and **37%HCHO@JNU-101**(cyan).

Characterization Section

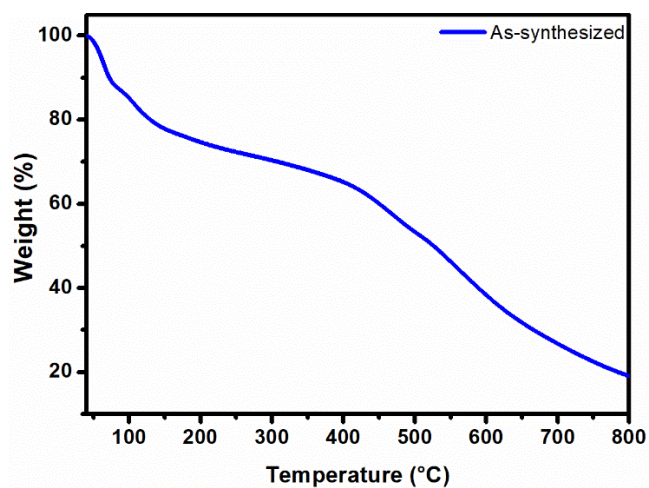


Figure S9. TGA of JNU-101.

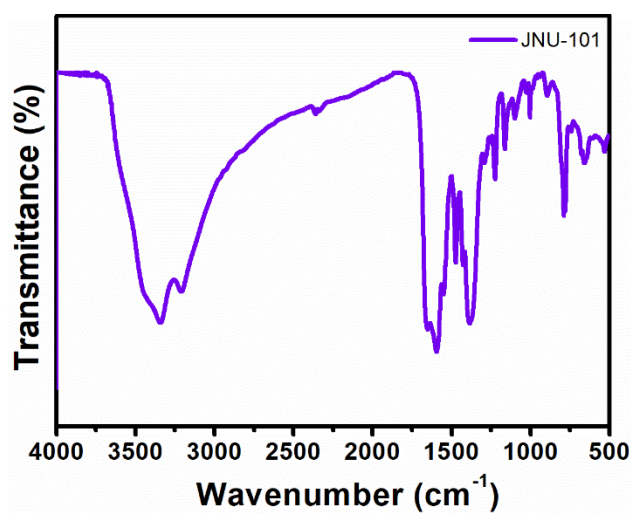


Figure S10. IR spectrum of JNU-101.

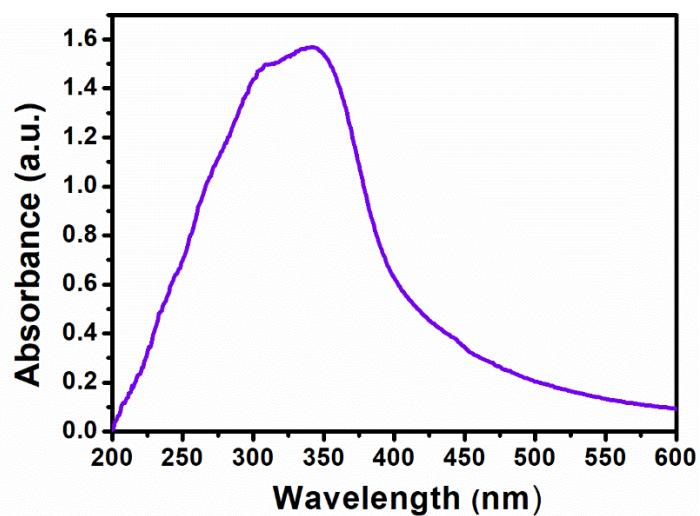


Figure S11. Solid-state UV absorption spectra of JNU-101.

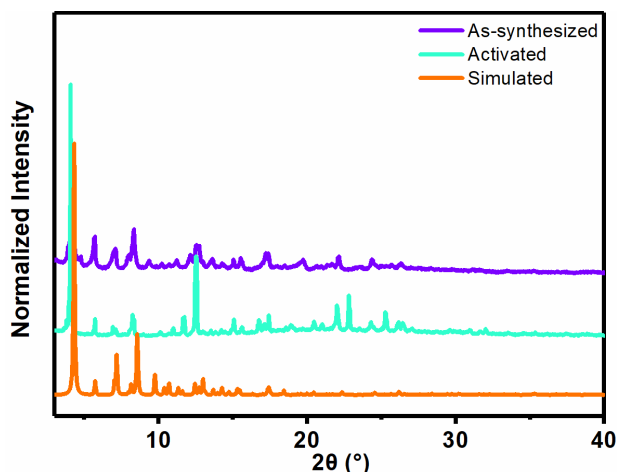


Figure S12. PXRD patterns of JNU-101.

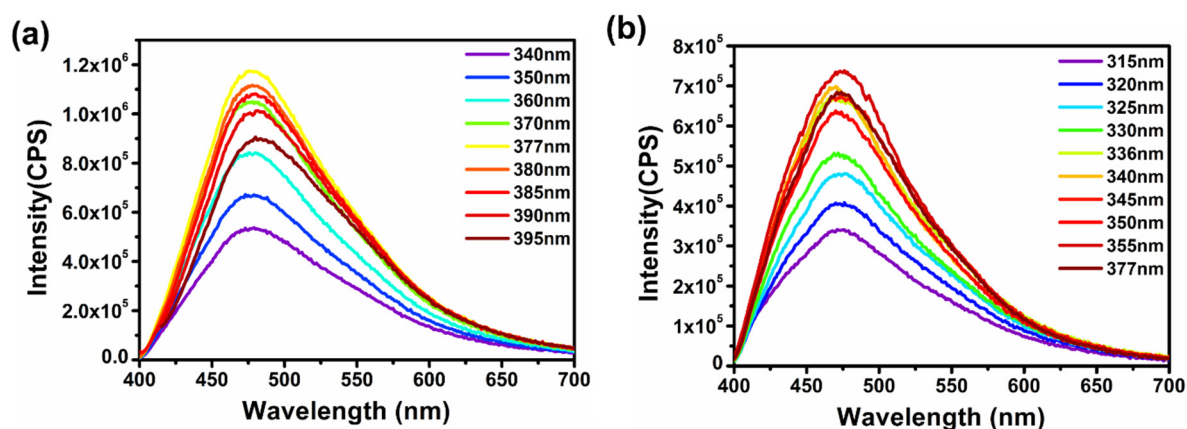


Figure S13. Excitation-energy-varied emission spectra of JNU-101 in (a) solid-state and (b) aqueous suspension.

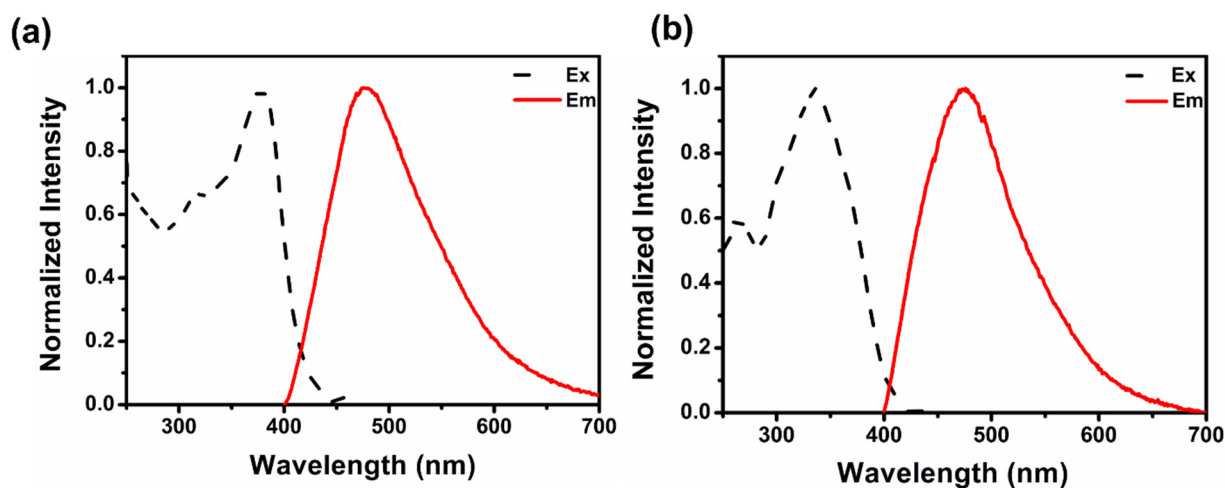


Figure S14. (a) Excitation and emission spectra of JNU-101 in solid-state with optimal excitation wavelength at 380 nm and emission wavelength at 477 nm. (b) Excitation and emission spectra of JNU-101 in aqueous suspension with optimal excitation wavelength at 336 nm and emission wavelength at 477 nm.

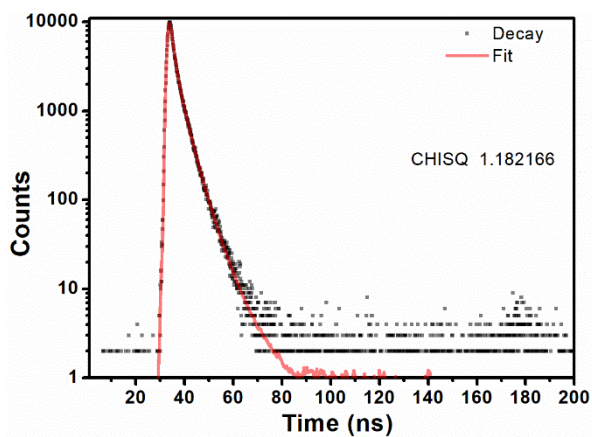


Figure S15. Fluorescence lifetime measurements for **JNU-101** in solid-state.

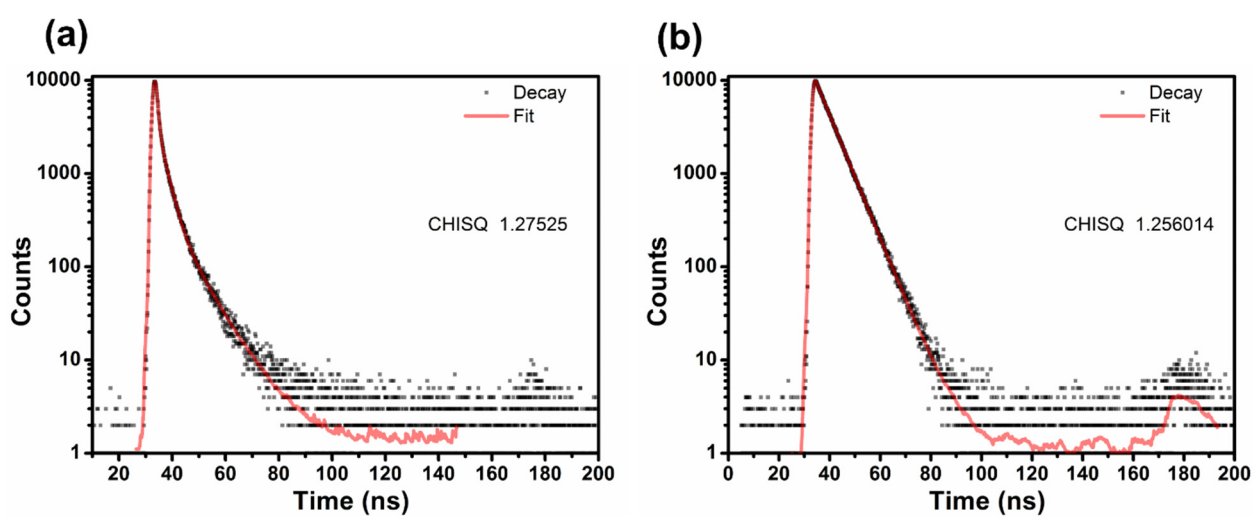


Figure S16. Fluorescence lifetime measurements for **JNU-101** suspension (0.20 mg mL^{-1}) (a) and upon addition of HCHO (0.10 M) at room temperature (b).

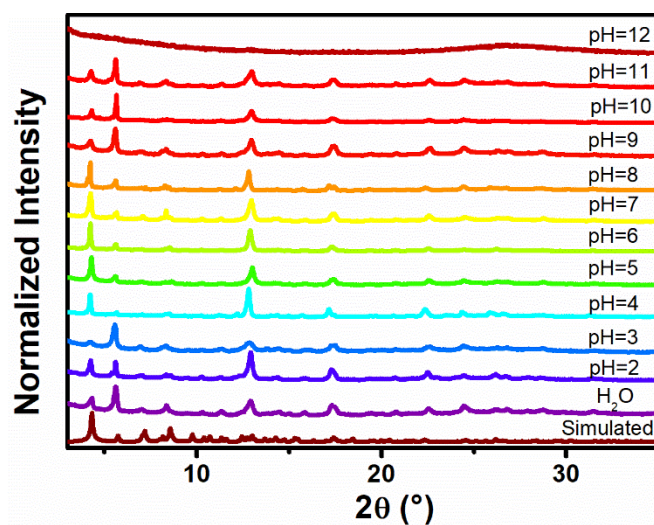


Figure S17. PXRD patterns of **JNU-101** after being soaked in acidic and alkali solutions for 7 days.

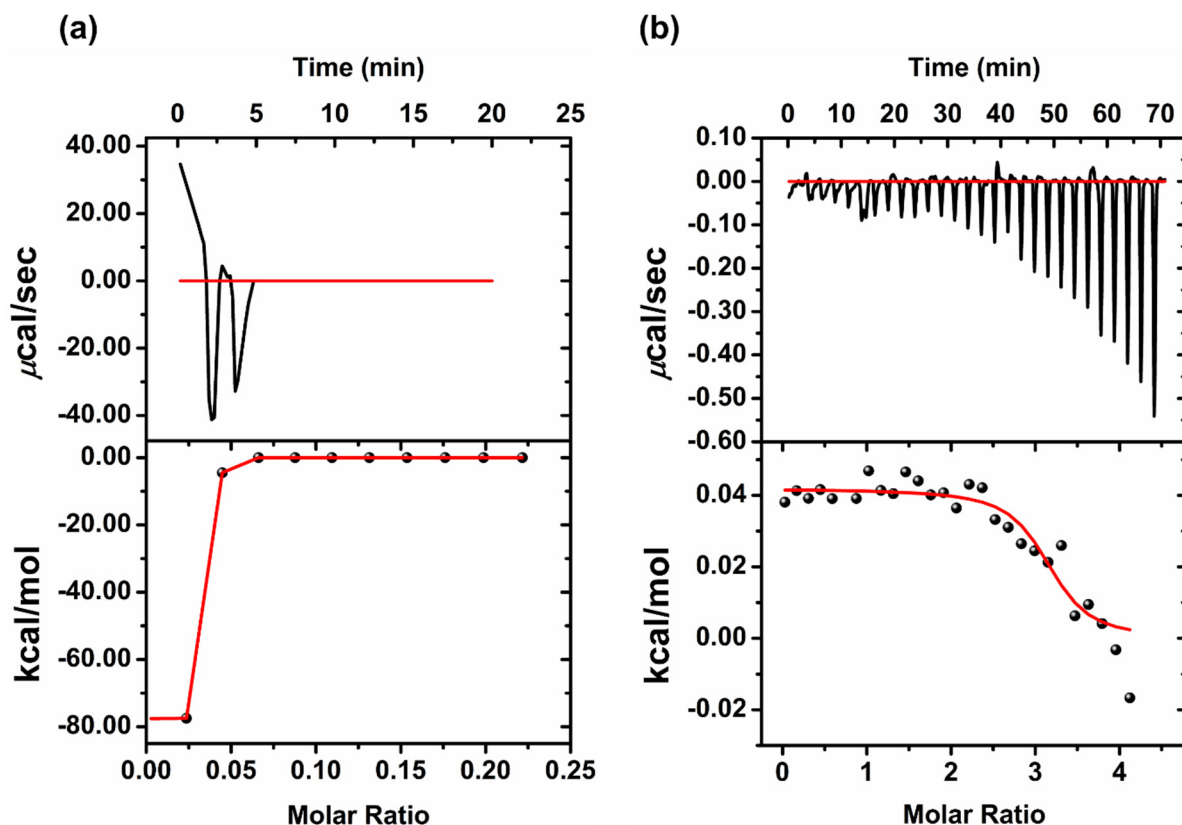


Figure S18. ITC thermograms for (a) titration of JNU-101 suspension (0.50 M) with H₂O and (b) titration of H₂O with HCHO (0.02 M).

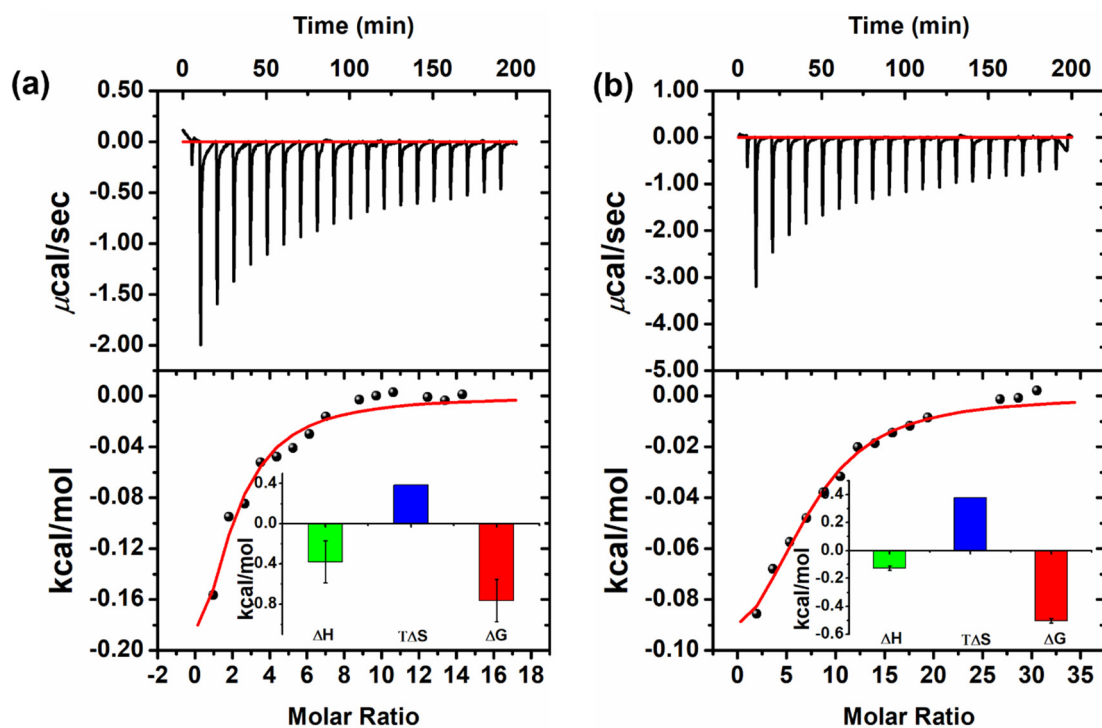


Figure S19. ITC thermograms for titration of a suspension of Zn(NO₃)₂·6H₂O, DAP, and H₂BPDC-2NH₂ mixture with (a) HCHO (50 mM, 300 μL), and (b) HCHO (100 mM, 300 μL). 12 μL each injection.

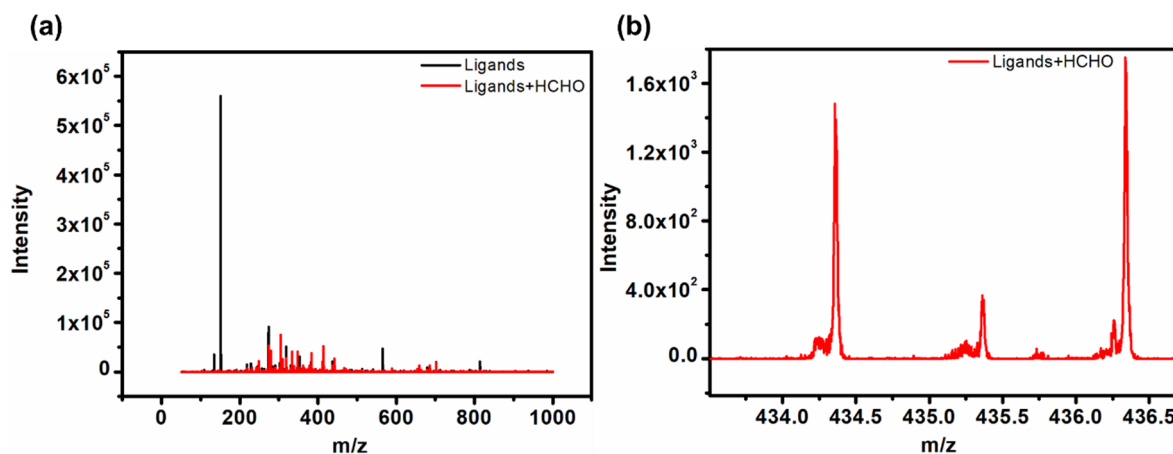


Figure S20. (a) HR-ESI-TOF-MS spectra of CH₃CN solutions of DAP and H₂BPDC-2NH₂ (black line, term Ligands) and treated with 37% HCHO (red line, term Ligands + HCHO). (b) Blow-up view of the red line in the range of 434 to 437 m/z.

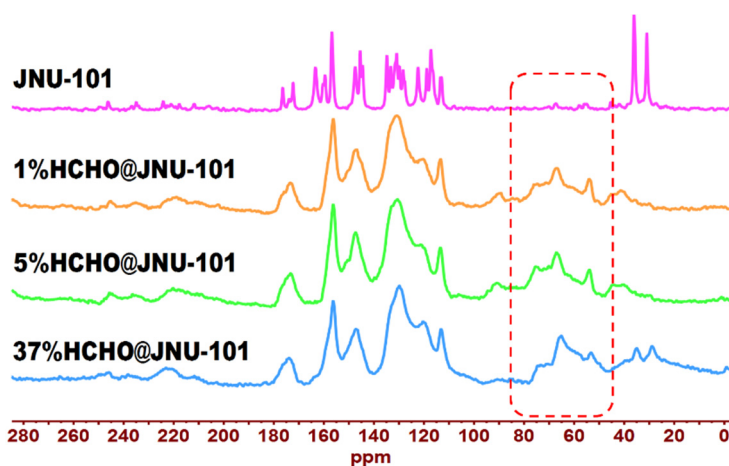


Figure S21. ¹³C-SSNMR analysis highlighting the characteristic carbon signals of aminoacetals.

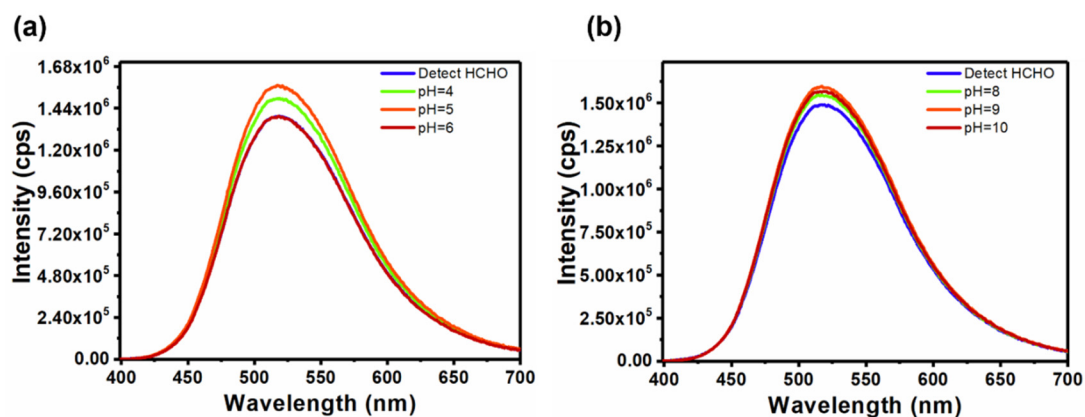


Figure S22. Fluorescence spectra of JNU-101 suspensions upon addition of HCHO (0.10 M) under (a) acidic conditions and (b) alkaline conditions.

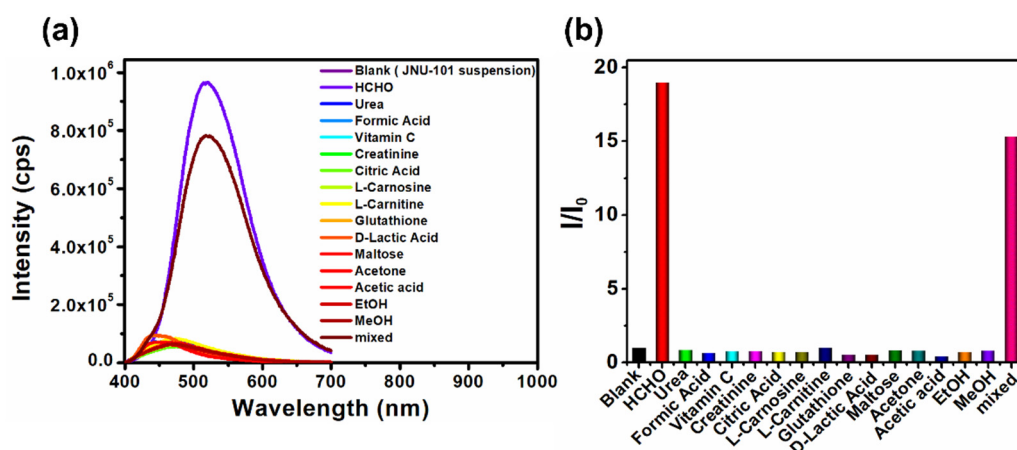


Figure S23. (a) Fluorescence emission spectra for JNU-101 suspension (0.20 mg mL^{-1}) upon addition of a variety of metabolites (0.10 M); and (b) comparison of their corresponding emission intensity ratio I/I_0 (I_0 = emission intensity of JNU-101 suspension).

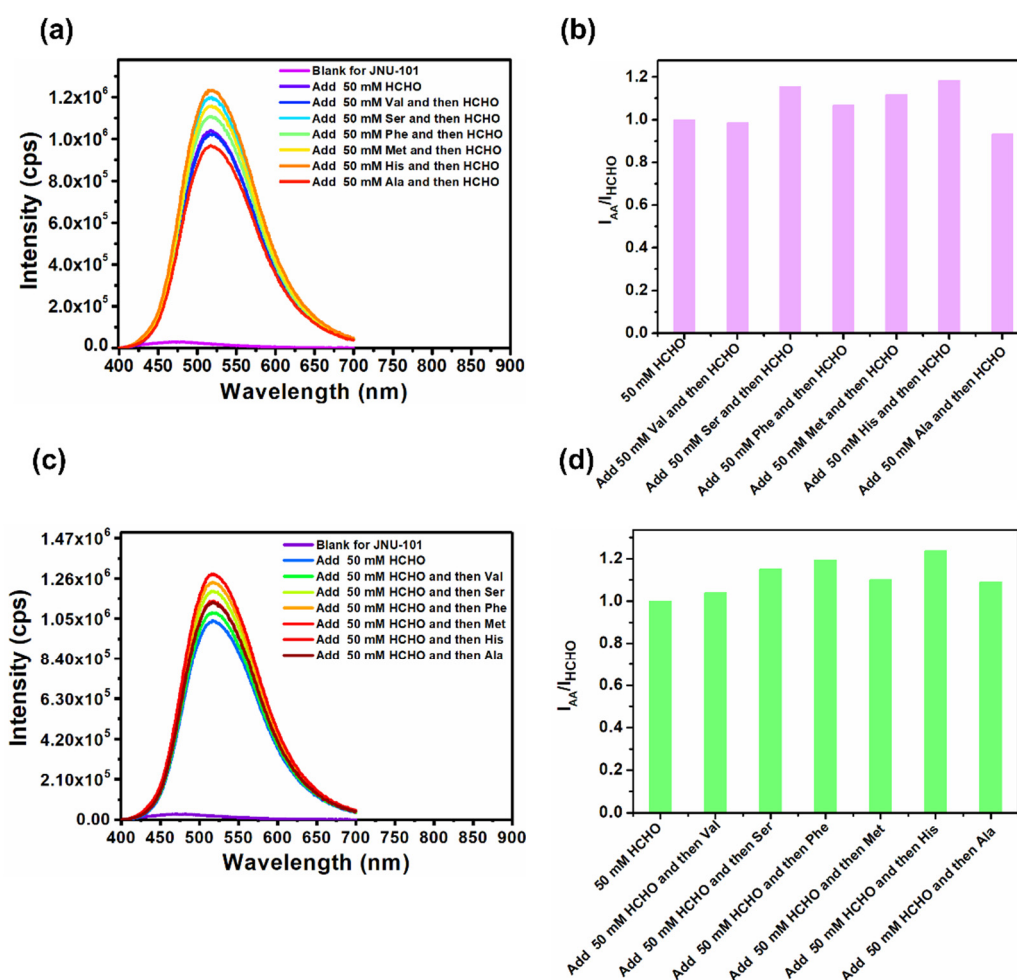


Figure S24. Fluorescence spectra of JNU-101 suspensions upon addition of different amino acids.

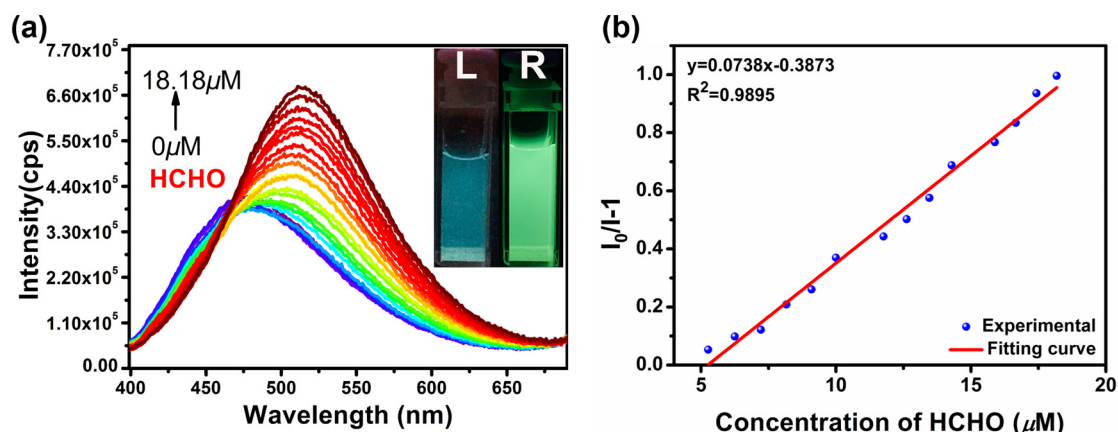


Figure S25. (a) Fluorescence emission spectra of **JNU-101** suspension (0.20 mg mL^{-1}) excited at 365 nm upon the incremental addition of HCHO. (b) The corresponding linear relationship between $I_0/I-1$ and the HCHO concentration from the concentration-dependent fluorescence titration experiments (a linear correlation was observed in the range of $5.26 \sim 18.18 \mu\text{M}$). The standard deviation (σ) of blank experiments was determined to be 0.001621, and the limit of detection (LOD) of **JNU-101** for HCHO in aqueous solution was thus calculated to be $0.066 \mu\text{M}$ (equivalent to 1.98 ppb) by using the formula $\text{LOD} = 3\sigma/k$ (k is 0.0738, the slope of the linear Stern-Volmer equation).

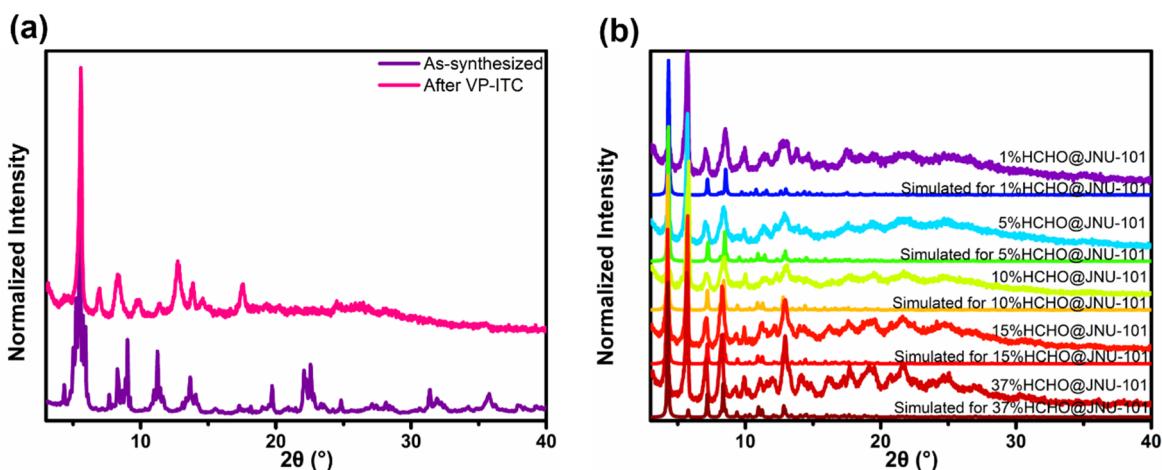


Figure S26. (a) PXRD patterns of **JNU-101** after ITC experiments, (b) PXRD patterns of **1% HCHO@JNU-101**, **5% HCHO@JNU-101**, **10% HCHO@JNU-101**, **15% HCHO@JNU-101**, and **37% HCHO@JNU-101**.

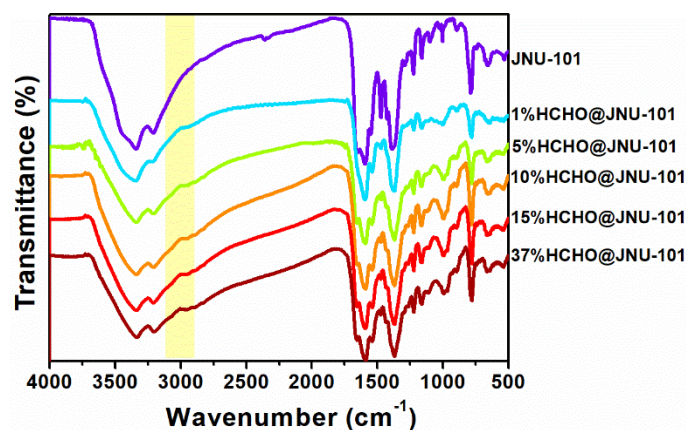


Figure S27. IR spectra of **JNU-101**, **1%HCHO@JNU-101**, **5%HCHO@JNU-101**, **10%HCHO@JNU-101**, **15%HCHO@JNU-101**, and **37%HCHO@JNU-101**.

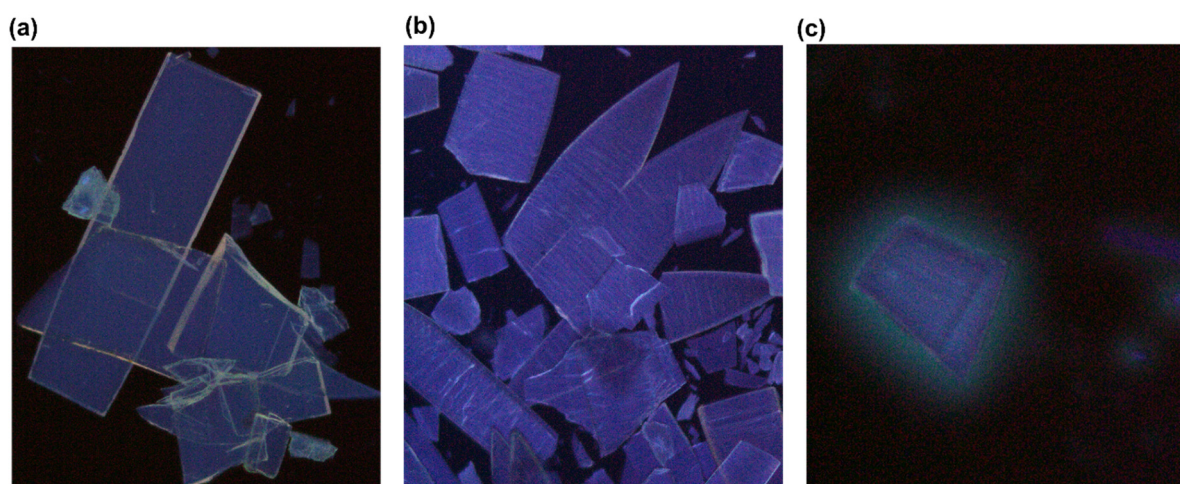


Figure S28. Fluorescence optical images of **JNU-101** in darkfield under UV irradiation after being incubated in culture medium (DMEM + 2% FBS) containing different concentrations of HCHO for 10 min. (a) 0.10 mM HCHO, (b) 0.20 mM HCHO, and (c) 0.40 mM HCHO.

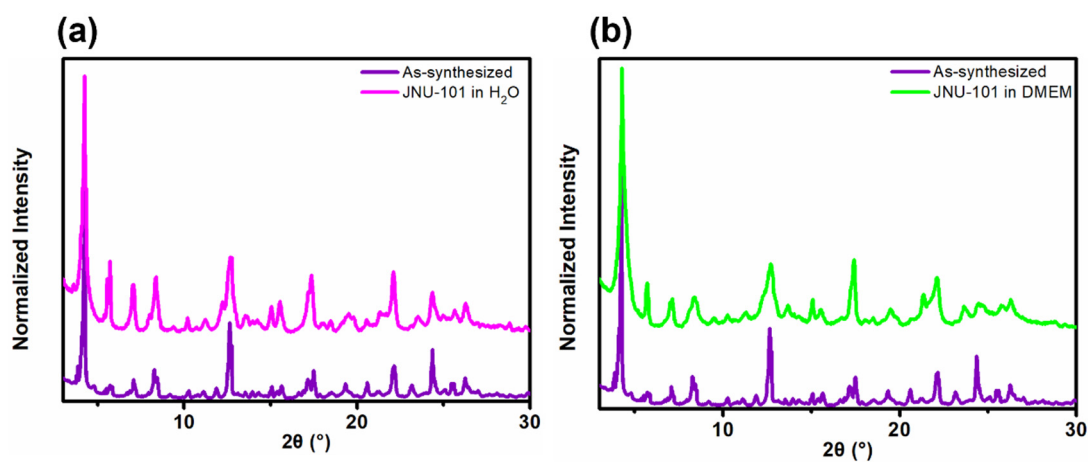


Figure S29. Comparison of PXRD patterns of **JNU-101** after being soaked in H₂O (a) and in DMEM solution (b).

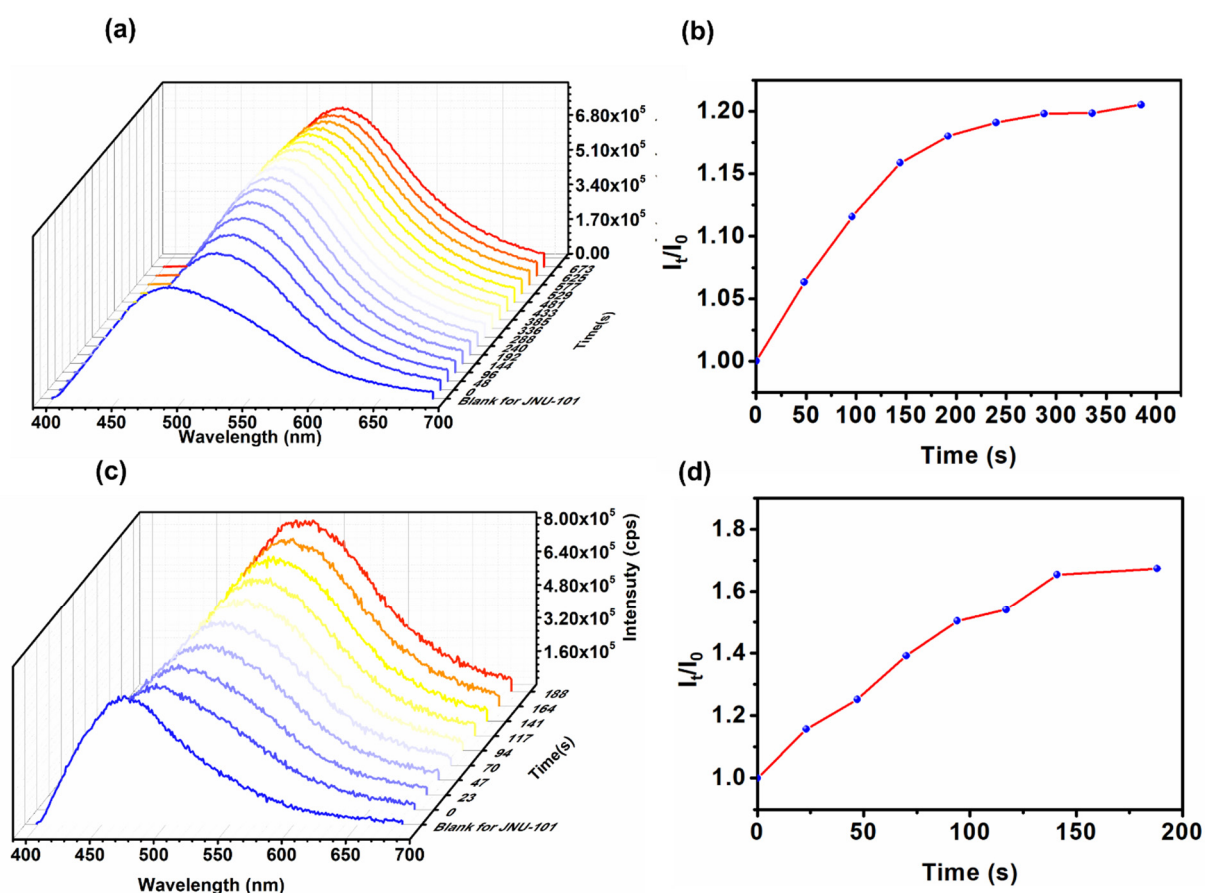


Figure S30. Real-time fluorescence monitoring of JNU-101 in the vapor phase over 1% HCHO aqueous solution at different time intervals. (a) 0.1 s, (c) 0.01 s. (b), (d) The corresponding plots of fluorescence intensity ratio (I/I_0) as a function of time.

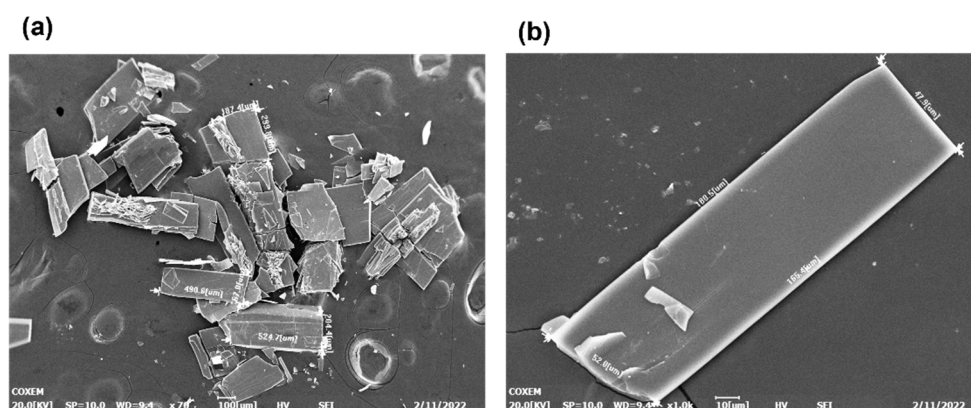


Figure 31. SEM images of JNU-101 crystals. The as-synthesized JNU-101 crystals show flake-like morphology with edges in the range of dozens to hundreds of microns based on SEM images. For example, $47.9 \times 165.4 \mu\text{m}^2$; $204.4 \times 524.7 \mu\text{m}^2$.

Notes and References

1. Y.-B. Wei, M.-J. Wang, D. Luo, Y.-L. Huang, M. Xie, W. Lu, X. Shu and D. Li, Ultrasensitive and highly selective detection of formaldehyde via an adenine-based biological metal–organic framework. *Mater. Chem. Front.*, 2021, **5**, 2416-2424.
2. J.-H. Wang, M. Li and D. Li, A dynamic, luminescent and entangled MOF as a qualitative sensor for volatile organic solvents and a quantitative monitor for acetonitrile vapour. *Chem. Sci.*, 2013, **4**, 1793-1801.